A Thesis

On

Synthesis of AFe_2O_4 (A=Fe, Mn, Co) nanoparticles for the magnetic hyperthermia treatment of Cancer

Submitted in partial fulfillment of the requirement for the award of the degree of

Master of Science

In

Physics

Submitted by

Abhishek Chandel

(302004001)

Under the supervision

of

Dr. B.N. Chudasama

(Professor)

Submitted to

School of Physics and Materials Science
Thapar Institute of Engineering and Technology
Patiala

July 2022

Dedicated to my Family

Declaration

I hereby declare that the dissertation entitled " **Synthesis of AFe_2O_4 (A=Fe, Mn, Co) nanoparticles for the magnetic hyperthermia treatment of Cancer** " is an authentic record of my work carried out as requirement for the the award of the degree of **Master of Science** at **Thapar Institute of Engineering and Technology, Patiala** under the supervision of **Dr. Bhupendra Kumar Chudasama** Professor, School of Physics and Materials Science, Thapar Institute of Engineering and Technology, Patiala. No part of the matter embodied in this dissertation has been submitted to any other university or institute for the award of any degree.

Date: 27/07/2022 (Abhishek Chandel)

302004001

It is certified that the above statement made by the student is correct to the best of my knowledge and belief.

(Dr. B.N. Chudasama)

Supervisor

Professor

TIET, Patiala

Acknowledgment

I would like to acknowledge and give my warmest thanks to my research supervisor **Dr. Bhupendra Kumar Chudasama**, Professor, Thapar Institute of Engineering and Technology, Patiala. Foremost, I am extremely thankful to **Mrs. Yashpreet**, research scholar, without her assistance and dedicated involvement in every step throughout the process, this dissertation would have never been accomplished. I would like to thank you very much for your support and understanding.

I am highly obliged to **Dr. Kulvir Singh**, Head of Department, School of Physics and Materials Science and **Dr. Maninder Singh**, Dean of academic affair for their guidance during various stage of this work. I want to embrace this opportunity to acknowledge my gratitude towards all the faculty members of the School of Physics and Materials science who were always accessible and helpful.

(Abhishek Chandel)
302004001

Contents

List of Figures **Page number**

List of Tables **Page number**

Abstract

With 10 million deaths in 2020 cancer remains one of the most challenging diseases in contemporary medicine. Chemotherapy, surgery, and radiation therapy severely harm healthy tissues and succeed rarely in advance stages of cancer. Recent studies indicate that magnetic hyperthermia, which involves targeted delivery of magnetic nanoparticles to tumor cells followed by localized remote heating of cancer tissues could revolutionize clinical practice in the treatment of cancer, either as standalone intervention or adjunct to radiotherapy or chemotherapy. Water dispersible magnetic nanoparticles (MNPs) of ferrites (AFe_2O_4; A=Fe, Mn, Co) are the promising candidates for magnetic hyperthermia due to their high chemical stability, biocompatibility, moderate magnetization and high specific absorption rate (SAR). In this thesis, magnetic hyperthermia efficiency of water based magnetic fluids of AFe_2O_4 (A=Fe, Mn, Co) nanoparticles is evaluated. AFe_2O_4 (A=Fe, Mn, Co) nanoparticles were synthesized by chemical co-precipitation method. Nanoparticles were coated with a bilayer of oleic acid and dispersed in water. Nanoparticle concentrations in magnetic fluids were 70 mg/mL for Fe_3O_4, 200 mg/mL for $MnFe_2O_4$ and 60 mg/mL for $CoFe_2O_4$. Structural and magnetic properties of MNPs were investigated by X-Ray diffraction (XRD) and vibrating sample magnetometer (VSM), respectively. XRD study revealed that AFe_2O_4 nanoparticles (NPs) exhibits cubic inverse spinel structure. Synthesized nanoparticles are soft ferromagnetic with very narrow hysteresis loops. Magnetic hyperthermia study was carried out as a function of magnetic field strength (2-10 mT) and field frequency (162-935.6 kHz) for 10 minutes. MNPs exhibits highest SAR values for 10 mT field strength at 935.6 kHz. Amongst the tested MNPs, Fe_3O_4 possess the highest SAR value (27.35 W/g), followed by $MnFe_2O_4$ (1.91 W/g) and $CoFe_2O_4$ (0.94 W/g). Considering this, it is concluded that amongst the studied inverse spinel ferrite nanostructures AFe_2O_4 (A=Fe, Mn, Co), Fe_3O_4 nanoparticles are most suitable for magnetic hyperthermia applications.

1.1 Nanotechnology and Cancer

Cancer nanotechnology is developing as a new area of interdisciplinary research that spans across fields of biology, chemistry, engineering and medicine. Nanotechnology has the aim of generating biocompatible materials, devices and systems that have unique properties due to their small size [1]. In order to create and control objects at the nanoscale size, nanotechnology manipulates matter at the atomic, molecular, and macromolecular levels. [2]. It entails creating materials or technologies that fit inside this size range and deals with materials that have dimensions between 1-100 nm [3].

One of the most important technologies for the future is nanotechnology. This is because materials can possess superior properties when reduced to the nanoscale than they do at the macroscale. At nanoscale, matter can display remarkable physical, chemical, and biological properties. As their size or structure is changed, they become more reactive, reflect light better and can be used for medical applications [4].

Nearly 10 million peoples died from cancer worldwide till 2020, making it the top cause of death. Cancer is a disease that is intrinsically biological and occurs when cell reproduction, a characteristic of all living things, gets uncontrolled. The World Health Organization (WHO) reports that cancer is leading cause of death. [5]. People of various ages, socioeconomic classes, and races may be affected by cancer, and it can develop anywhere in the body [5]. Common treatments of cancer are surgery, chemotherapy and radiation therapy, which are in general harmful to the healthy cells. These therapies are rarely successful if the cancer is in the advance stage. Due to the unique benefits of nanoparticles like high biocompatibility, excellent stability, high permeability and retention, and precision targeting; they can be utilized for the treatment of cancer. When compared to other treatments, nanoparticle based therapy has numerous advantages, including being target-specific, minimally invasive, and having very less adverse effects [6].

1.2 Cancer treatments

The American Cancer Society (ACS) lists surgery, radiation therapy, chemotherapy, immunotherapy, targeted therapy, etc. as frequent cancer therapies.

1.2.1 Surgery

Surgery is a technique used to remove a tumor and adjacent tissues. It is the oldest cancer therapy still quite effective against variety of cancers [7]. Solid tumors that are localized within the human body respond best to surgery. It is a localized treatment that solely targets the body portions with cancer. Cancers that have spread to several body organs cannot be treated with surgery. The extensive list of limitations associated with surgery includes organ loss, a prolonged healing process, and a high recurrence rate.

1.2.2 Radiation therapy

Radiation therapy, often known as radiotherapy, uses high radiation doses to destroy cancer cells and shrink tumors. Radiation therapy damages cancer cell's DNA, which either kills them or stops their growth. Cancer cells that can no longer divide due to DNA damage eventually cease growing and die. The body expels the injured cells once they are dead. Cancer cells are not instantly destroyed by radiation therapy. Before enough DNA is broken to cause cancer cells to die, it may take days or weeks of treatment [8]. Radiation therapy also has an impact on healthy tissues. Damage to healthy cells has negative side effects that compromise the life quality of the patient.

1.2.3 Chemotherapy

Drugs are used during chemotherapy to eradicate cancer cells. Chemotherapy may be the only viable treatment in many cases. Chemotherapy is typically used in conjunction with other cancer treatments. The necessary forms of treatment vary depending on the type of cancer, where it has spread, and underlying health issues. Chemotherapy side-effects include exhaustion, an increased risk of infection, nausea and vomiting, lack of appetite, diarrhea, etc. Once the treatment is over, these adverse effects typically disappear [7]. Like other cancer treatments, it rarely works if the cancer is in advance stage.

1.2.4 Immunotherapy

A cancer treatment known as immunotherapy encourages the patient's immune system to attack the disease. Infections and other ailments are fought off because of this. It is used as supplementary treatment along with chemotherapy and radiation therapy. Skin response at the injection site is the most common side-effect. Along with this, other side effects like discomfort, infection, diarrhea, itching, etc. are also prevalent [8].

1.2.5 Photodynamic therapy

The term photodynamic therapy (PDT) is sometimes used to refer to phototherapy, photo radiation therapy or photo chemotherapy. In order to kill cancer cells, this treatment combines special medications called photosensitizers with light. Only after being exposed to radiation do these medications start to work. The photosensitizers are either injected into the bloodstream or implanted beneath the skin, depending on the area of the body being treated. The cancer cells take up the medication. The treated tissue is then exposed to light. Reactive oxygen species (ROS), which damage cancer cells, are released when the medication reacts with oxygen [9]. PDT might also act by obliterating the blood arteries that supply cancer cells with nutrients and by igniting the body's defense mechanisms to fight the malignancy. PDT has the limitation that it can only treat tissues or organs that can receive light. This indicates that it is mainly employed to treat tumors that are located on close beneath or within the lining of internal organs. The major limitation of this therapy is days after the procedure, the patient remains photosensitive.

1.2.6 Hyperthermia

In order to treat cancer with hyperthermia, body or tissue temperature is raised. The body temperature is elevated above normal for a predetermined time in hyperthermia, which can affect either a portion or the entire body. The degree of temperature elevation linked to hyperthermia is of the order of a few degrees (41–45 °C) over the average body temperature. Due of their low heat tolerance, cancer cells can be killed by rising temperatures with minimal damage to the normal tissues [10].

1.3 Types of hyperthermia treatment

1.3.1 Regional Hyperthermia

The use of external array of applications to provide heat to a sizeable portion of the body or more specially a whole organ is the method used in this case. Progressive heat distribution is the norm. A portion of blood is extracted via a procedure called “regional perfusion hyperthermia” returned into the patient’s body after being heated and pushed out of it [15].

1.3.2 Whole-body hyperthermia

This method involves heating the entire body to a minimum temperature of 41°C. In this

process, hot wax, hot water blankets or inductive loops are used to heat the entire body on the surface.

1.3.3 Local Hyperthermia

Local hyperthermia therapy is applied to relatively tiny tumors that are close to the body's surface. This method concentrates the distribution of heat. Applicators are inserted under the skin of a superficial cancer or implanted into the intended location to transmit electromagnetic waves like radio, microwave, or ultrasound to induce localized heating [15].

1.4 Hyperthermia Mechanism

Compared to physiological settings, hyperthermia promotes oxygenation of tumors and tissues. Variation in tumor blood flow (TBF) appears to be the primary mechanism by which the oxygenation of the tumor changes during hyperthermia. Temperature higher than 42 ℃ cause TBF to decrease, causing the start of cell death in cancer tumors. Moderate hyperthermia (39-41 ℃) increases TBF. At 45 ℃, cell death also occurred in healthy tissues as a result of a significant reduction of nutritive blood flow brought on by the shutdown of microcirculation. Hence, the therapeutic temperature window is defined as 41–44 ℃ [16].

1.5 Magnetic Hyperthermia

In Magnetic hyperthermia, MNPs are exposed to an alternating magnetic field (AMF), which causes particular body parts to become hot (tissues or cells). Heat is generated by two mechanisms:

i. Hysteresis losses
ii. Relaxation losses.

1.5.1 Hysteresis losses

As current flows forward and backward, the core is magnetized and demagnetized, which results in hysteresis loss. As the magnetizing force (current) increases, the magnetic flux increases. However, the magnetic flux decreases less gradually and at a slower pace as the magnetizing force (current) is reduced. As a result, the flux density will remain positive even when the magnetizing force is zero. The flux density will reach zero when applying the magnetizing force in the opposite direction. The energy required to complete a full cycle of magnetization and demagnetization, as well as the energy wasted during this process, are

represented by the size of the hysteresis loop [11]. The relationship between the magnetizing force and the induced magnetic flux density (B) is depicted by a hysteresis loop (H) in Fig. 1.

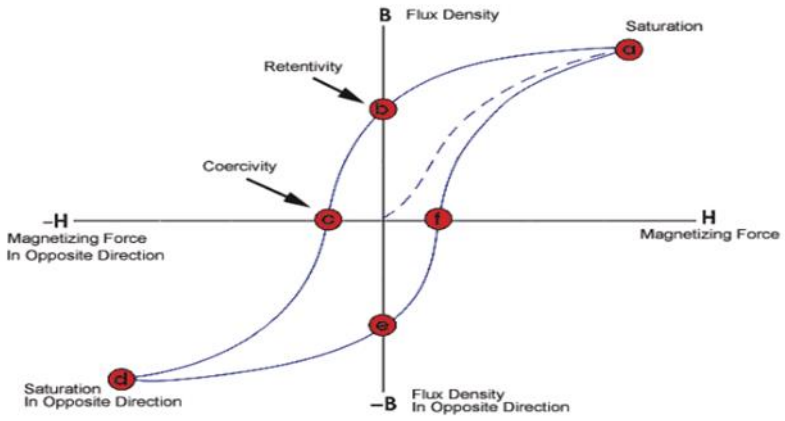

Fig. 1 Representative hysteresis loop of a magnetic material [11]

1.5.2 Relaxation Losses

Brownian Relaxation

If a magnetic nanoparticle is held in an alternating magnetic field, its magnetic dipole moment will align in the direction of the applied magnetic field.. In Brownian rotation the particle moment rotates physically when the field direction changes. This rotation of nanoparticles is referred as Brownian rotation.

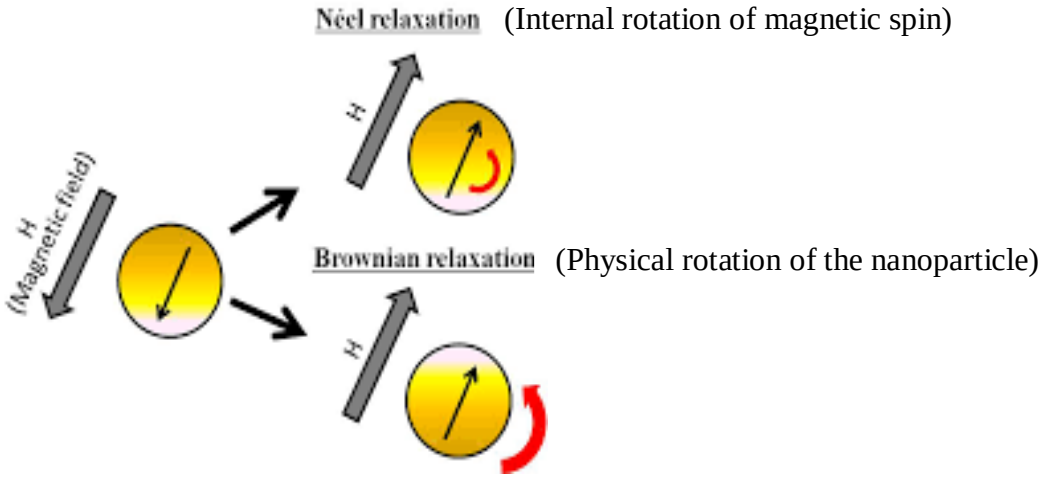

Fig. 2 Neel and Brownian relaxation [14]

Neel Relaxation

The particle moment moves in the direction of the field. Internal rotation of the particle's moment occurs when the field direction changes without the particle physically rotating. Both relaxations i.e., rotation of moment of particle with physical rotation and without physical rotation release their stored magnetic energy in the form of heat. These relaxation processes are summarized in Fig. 2.

1.6 Specific Absorption rate (SAR)

A measure of the heat-generating potential of magnetic nanoparticles is the specific absorption rate (SAR) or specific loss power (SLP), which is defined as the heat energy produced by the unit mass of magnetic particles. Studies investigating hyperthermia have employed SAR, or the mass-normalized rate of energy absorption by a biological organism, to describe the patterns of energy deposition and heating in tissues of biological models. The initial rate of temperature rise during heating is often utilized to calculate SAR. The most crucial element in hyperthermia is temperature. As described by SAR, [13]

$$\text{SAR or SLP (W/g)} = C\frac{\Delta T}{\Delta t}$$

Here C is the specific heat capacity of the colloid and $\Delta T/\Delta t$ is the rate of change of temperature. The specific absorption rate (SAR) value is significant for biomedical applications because a greater SAR of nanoparticles will result in a lower dose of nanoparticles being injected. The saturation magnetization and the volume fraction of magnetic nanoparticles have a significant impact on SAR.

1.7 Ferrites AFe_2O_4 (A=Fe, Mn, Co) for Magnetic Hyperthermia

The term "ferrites" refers to a class of oxides with ferric ions as its primary component. Ferrites have benefits such being applicable at higher frequencies, having more heat resistance, having greater corrosion resistance, and being less expensive even if their saturation magnetization is less than half that of ferromagnetic alloys. Due to their biocompatibility and long-lasting magnetic properties, nano ferrites are widely used in biomedical applications, particularly in magnetic hyperthermia treatments [12].

Based on how well they resist demagnetization (magnetic coercivity), ferrites can be classified into two categories;

1.7.1 Soft Ferrites

A soft magnetic substance with an iron-oxide base is called soft ferrite. They possess excellent high-frequency magnetic properties and good electrical resistance. Soft ferrites also possess low value of remanence and coercivity [15].

1.7.2 Hard Ferrites

High coercivity and remanence characterize hard ferrites. Barium, strontium carbonate, or iron oxide make up hard ferrites. Due to their high coercivity, these materials are particularly resistant to demagnetization, which is a necessary quality for permanent magnets. They are also highly magnetically permeable [15]. Magnetic properties of soft and hard ferrites are summarized in Fig. 3.

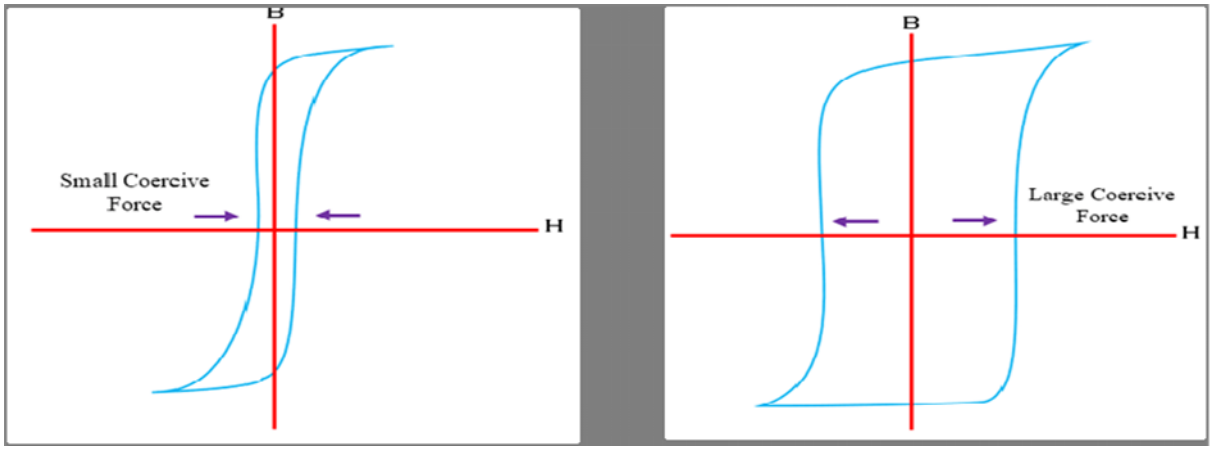

(a) **(b)**

Fig. 3 Hysteresis loop of (a) soft and (b) hard ferrites [31]

1.8 Superparamagnetism

Superparamagnetism is the magnetism of small ferrimagnetic or ferromagnetic nanoparticles. This effect happens when ferromagnetic or ferrimagnetic nanoparticles possess single magnetic domain. For most of the materials this happens below a particle size of 10 nm. In this case, thermal energy is sufficient to alter the crystallite's overall magnetization direction, despite the

temperature being below the Curie point. In the absence of an external magnetic field, nanoparticle magnetization appears to be zero, when the measurement period is significantly longer than the Neel relaxation time. [17].

In this form, magnetic fields from outside can magnetize the nanoparticles, which are otherwise acting as paramagnet. However, compared to paramagnets, their magnetic susceptibility is substantially high. Crystalline anisotropy energy is the energy needed to shift a crystallite's magnetization direction. This depends on the size of the nanoparticle. The crystalline anisotropy energy decreases together with the crystallite size, which lowers the temperature at which the substance becomes superparamagnetic. Superparamagnetic materials exhibit zero remanence and coercivity. To clearly understand the difference between a ferromagnetic material, a paramagnetic material and a superparamagnetic material, their hysteresis loops are presented in Fig. 4.

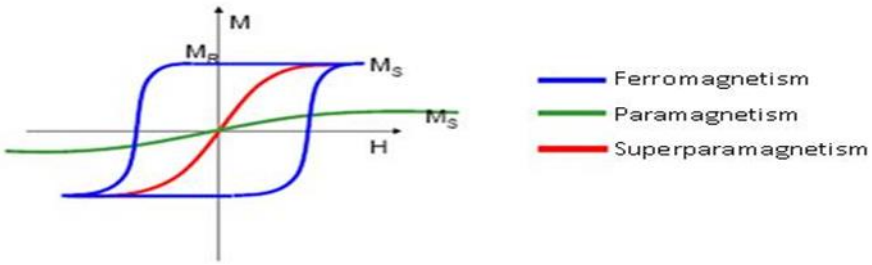

Fig. 4 Hysteresis loop showing ferromagnetism, paramagnetism and superparamagnetism [18]

Hoffmann et al. synthesized superparamagnetic iron oxide nanoparticles by chemical co-precipitation. The polymer coating of polyvinyl alcohol was used to stabilize nanoparticles. The hydrodynamic size varies between 50 to 80 nm. In-situ production of iron oxide nanoparticles coated in polyvinyl alcohol is followed by their implantation in a silica matrix. The specific loss power (SLP) in a 6 mT AC magnetic field at 140 kHz is 7.7 W/g. This SLP number is high enough to kill tumor with a 4 cm diameter at temperatures higher than 42°C [23].

Drake et al. reported Gd doped iron oxide nanoparticles synthesized for tumor treatment using magnetic fluid hyperthermia. The composition of nanoparticles was $Gd_{0.02}Fe_{2.98}O_4$ and particle size measured through TEM was ~13 nm. The specific absorption rate measured with 246 Oe at 52 kHz was 36 W/g. The mouse model treated by these nanoparticles shows slower tumor growth as compared to Fe_3O_4 [24].

Bonder et al. synthesize biocompatible carboxyl-terminated polyethylene glycol coated iron oxide nanoparticles [IONPs]. They have average size of 10 nm. IONPs exhibit high saturation magnetization and permits effective heat generation in the safe frequency range. By applying a 4 Oe magnetic field at a frequency of 500 kHz to a sample of IONPs dispersed in ethyl alcohol (2 mL), heating effects were investigated. Particles shows good dispersion for 20 minutes which is sufficient to perform hyperthermia studies [25].

Soares et al. reported synthesis of superparamagnetic iron oxide nanoparticles and a bilayer coating of oleic acid is done. At neutral pH, the most stability was accomplished. By using transmission electron microscopy (TEM) size of iron oxide-cored NPs dispersed in water with an oleic acid bilayer had an average diameter of 9 nm. About 170 nm was the hydrodynamic diameter. Fe_3O_4 nanoparticles are very stable. The application of an AC magnetic field results in the expected heating of the NPs. [26].

Ebrahimisadr et al. investigated the impact of nanoparticle concentration on the magnetic hyperthermia characteristics of Fe_3O_4 nanoparticles. Nanoparticles are synthesized by co-precipitation and the mean particle diameter is ~ 18 nm. With the aid of an induction heater that produces an alternating magnetic field with a frequency of 92 kHz, the hyperthermia

properties of Fe_3O_4 nanoparticles was studied. The maximum temperature rise is 58 °C for the sample with a concentration of 12.5%, and the lowest rise is 9 °C, for a concentration of 1%. SAR values determined by the two alternative methods, Box-Lucas and linear fitting of temperature vs. time curves shows that concentration has very little impact on SAR value of Fe_3O_4 nanoparticles [27].

Bani et al. investigated the heating properties of casein-coated magnetic iron oxide nanoparticles under an alternating magnetic Field. Magnetic nanoparticles are synthesized via one pot chemical method. Average core size determined by TEM is 20-25 nm. VSM study shows the superparamagnetic nature of coated and uncoated iron oxide nanoparticles. Hyperthermia tests were done with casein coated MNPs with various concentrations and frequencies. Highest SAR (22 W/g) was recorded at a concentration of 1 mg/mL and at 150 kHz frequency [28].

Amighian et al. synthesized Mn ferrite nanopowders by co-precipitation method. Temperature studies show that a mixture of the nanoparticles and distilled water (10 g/L) in the presence of an AC magnetic field (f=400 kHz) can produce a temperature increase of up to 5 °C after 20 minutes.. Given that the nanoparticles are smaller than 10 nm in size, heat produce may be because of Neel relaxation losses [29].

Doaga et al. synthesized $Mn_xFe_{1-x}Fe_2O_4$ ferrite nanoparticles with *x* ranging between 0 and 1. Co-precipitation was used to prepare manganese ferrites nanoparticles. X-ray study showed that the crystallite size is in the nanometer range and it increases with the degree of Mn cation substitution. Average particle size of nanoparticles obtained from TEM was ranging between 10.5 and 19 nm. The hydrodynamic diameter of water dispersed nanoparticles was ranging between 60-105 nm. Nanoparticles were superparamagnetic. Highest value of 148.4 W/g of SAR was registered for $MnFe_2O_4$ at 4500 A/m field. Measurements at 1.95 MHz frequency and with increasing field upto 2300 A/m have proved a proportional increase of the SAR values, from 68.7 to 103.4 W/g. $Mn_xFe_{1-x}Fe_2O_4$ nanoparticles may be effective for hyperthermia applications due to their exceptional thermal characteristics and potential biocompatibility [30].

Patade el al. synthesized different zinc concentrations in manganese ferrite by chemical coprecipitation technique. As zinc concentration rises, the average crystallite size decreases from 18 to 12 nm. Synthesized nanoparticles are superparamagnetic. An induction heating system was used for the magnetic hyperthermia study. At 4.0 kA/m, $MnFe_2O_4$ and $Mn_{0.3}Zn_{0.7}Fe_2O_4$ nanoparticles (2 mg/mL) may each reach 42 °C in 267 seconds and 563 seconds respectively? The results demonstrate that the SAR values of MnFe2O4 and Mn0.7Zn0.3Fe2O4 are, respectively, 217.62 W/g and 170.88 W/g. [31].

Mazario et al. synthesized citric acid coated cobalt ferrite nanoparticles of two different sizes (13 and 28 nm) and dispersed them in water. Specific absorption rate were determined at 32 and 101 kHz frequency at 51 mT field. SAR value of 28 nm particles is higher than 13 nm particles. Despite using an amine surfactant to create the nanoparticles, the resulting material lacks the stability needed for biomedical applications. This calls for the use of a fresh stabilizing chemical to raise their colloidal stability. The H_of product used in the present study was below the biological and physiological safety range in biomedical applications ($H_of < 5 \times 10^9$ A/ms), this implies that $CoFe_2O_4$ nanoparticles would be useful for applications using magnetic hyperthermia. [32].

Al Lehyani et al. synthesize cobalt ferrite nanoparticles by using chemical precipitation method. The powder that was produced underwent calcination at various temperatures (600°C, 800°C, 900°C, and 1000°C). The induction heater was made to be able to produce magnetic fields with high frequency and strength (8 kA/m, 135 kHz). The temperature increase (T) of the tube content at 60 seconds was 29.9 °C, 26.7 °C, 25 °C, and 22.9 °C, respectively, for MNPs of 18 nm, 26.7 nm, 25 nm, 60 nm, and 95 nm.. With a diameter of about 18 nm, the tiniest nanoparticles have a greater heating efficiency. The particle heating efficiency was increased by reducing the particle size in the alternating current from 95 nm to 18 nm [33].

From the above literature review we have concluded that ferrites have good structural and magnetic properties, which helps in generating heat for magnetic hyperthermia. Also the size plays an important role in magnetic hyperthermia. Ferrites are biocompatible, less toxic and they have a higher SAR which shows that with a low dose of nanoparticles magnetic hyperthermia treatment can be done. However, the reported SAR values of AFe_2O_4 (A=Fe, Mn, Co) nanoparticles varies too much and their dependence on magnetic field frequency and field strength are unknown. Hence in this thesis, we propose to investigate the magnetic

hyperthermia properties of AFe_2O_4 (A=Fe, Mn, Co) nanoparticles under diverse magnetic field conditions. Following objectives are proposed:

Objectives

- To synthesize AFe_2O_4 (A=Fe, Mn, Co) nanoparticles with a low crystallite size and high saturation magnetization.
- To investigate the effect of magnetic properties, size and size distribution on magnetic hyperthermia.
- To calculate the SAR values of synthesized ferrites at different fields and frequencies and to investigate the effect of concentration of nanoparticles on their magnetic hyperthermia performance.

Synthesis of AFe_2O_4 (A=Fe, Mn, Co) nanoparticles

The bottom-up technique and co-precipitation method is used to synthesize AFe_2O_4 (A=Fe, Mn, Co) nanoparticles. One of the best processes for creating ferrite nanoparticles is co-precipitation. It is a low cost and low temperature process.

3.1 Synthesis of Fe_3O_4 (Iron Oxide) nanoparticles

Materials:

Ferric chloride hexahydrate ($FeCl_3 .6H_2O$) obtained from HIMEDIA and ferric sulphate heptahydrate ($FeSO_4 .7H_2O$) obtained from LOBA Chemicals are used as precursors. NaOH is obtained from LOBA Chemicals. All aqueous solutions are prepared in Milli-Q ultrapure distilled water (ρ =18.2 MΩ)

Procedure:

All the precursors used are taken in the stoichiometric ratio of 1:2:8. Base fluid NaOH 0.8 mM (3.2 g) is prepared in 200 mL distilled water. Acids $FeCl_3.6H_2O$ 0.2mM (5.406 g) and $FeSO_4.7H_2O$ 0.1mM (2.780 g) are also prepared in 200 mL distilled water. Under the constant stirring acid solution is added to the base solution and pH is set to 11 within 10-15 seconds with the help of excess NaOH solution. The reaction was allowed to proceed for 20 minutes at room temperature. The following reaction takes place:

0.2 mM $FeCl_3.6H_2O$ + 0.1 mM $FeSO_4.7H_2O$ + 0.8 mM NaOH $\rightarrow$ 0.1 mM Fe_3O_4 + 0.6 mM NaCl + 0.1 mM Na_2SO_4 + 2.3 mM H_2O

The precipitates are of brown color. The resultant slurry is magnetically decanted, washed with warm distilled water three to four times, and then treated with acetone to eliminate any contaminants. After this, nanoparticles are dried overnight in oven at 60 ℃. The dried nanoparticles are then grinded using mortar pestle. Synthesis protocols followed here are summarized in Fig. 5 as a flow chart.

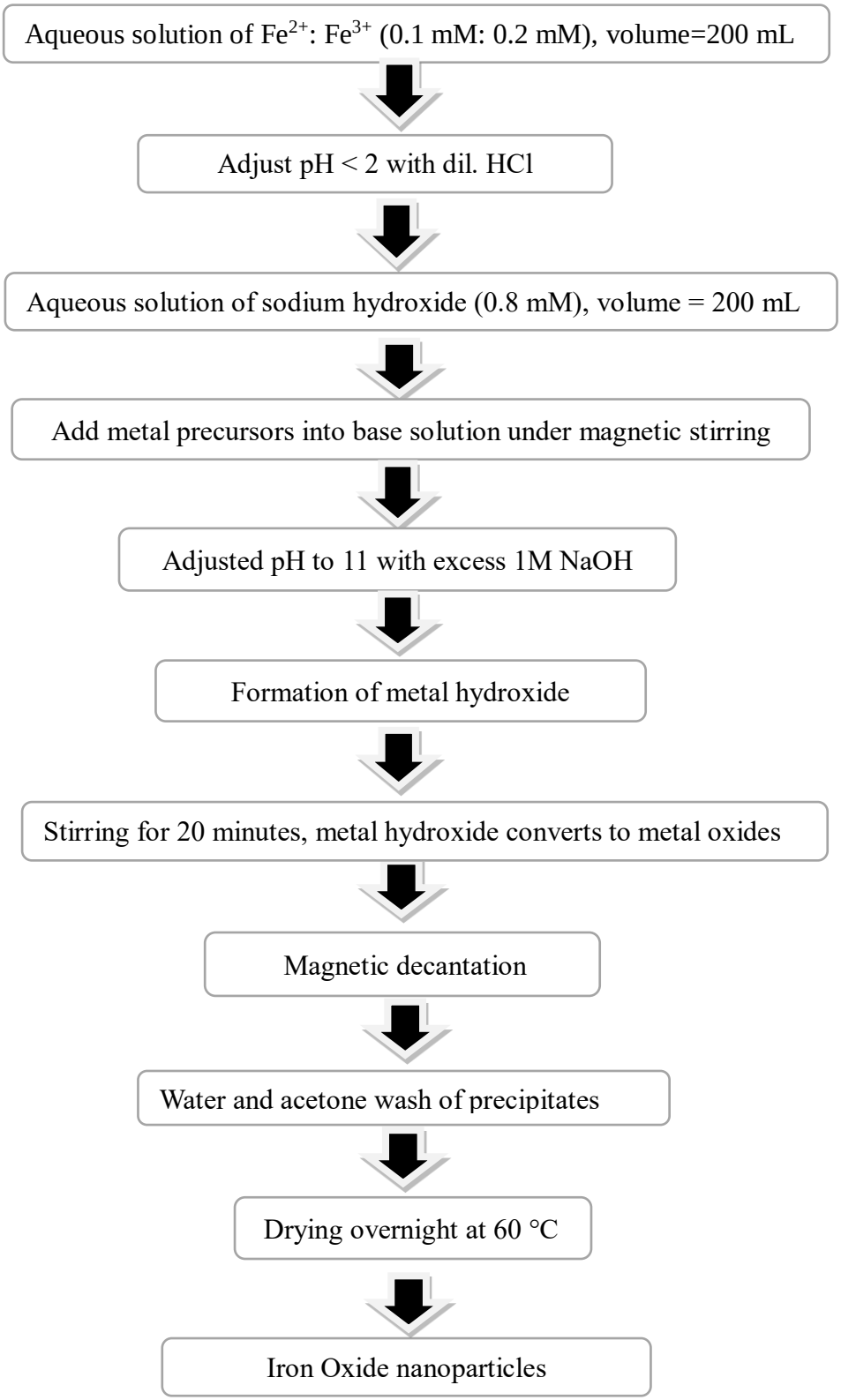

Fig. 5 Synthesis protocols for the preparation of Fe_3O_4 nanoparticles

Preparation of aqueous magnetic fluid of Iron oxide

Iron oxide (Fe_3O_4) nanoparticles are synthesized by following the protocols described in Fig. 5, till the washing step. After multiple water washes, iron oxide nanoparticles are dispersed in 100 mL distilled water. Under basic circumstances, 2.3 g of oleic acid was dissolved to produce 100 mL of sodium oleate solution. 100 mL dispersion of iron oxide nanoparticles was then added to the sodium oleate solution (100mL). It was stirred with the help of mechanical stirrer at room temperature for 2 hours. Following this it was heated to 90 °C for 2 minutes under continuous stirring. At this stage oleic acid binds to the surface of nanoparticles and stabilizes them by steric repulsion. Now the heating was turned off in order to allow the solution to cool to room temperature. Next to flocculate nanoparticles, solution pH was adjusted to <5 with the help of dil. HCl. It is then magnetically decanted and 3-4 times washed with warm distilled water. Following this slurry was washed with ethanol + acetone (100 mL). After this nanoparticles are dispersed in 10 mL distilled water with sonication. Additional 15 mL sodium oleate solution was prepared as per the protocols explained previously. To the oleic acid-coated Fe_3O_4 nanoparticle slurry, this sodium oleate solution was added drop by drop while being gently heated. Addition of oleic acid was continued drop - by - drop till the nanoparticles exhibits a complete suspension. Once they are fully suspended, addition of sodium oleate was stopped, to remove clusters of nanoparticles, if any; magnetic fluid thus prepared was subject to centrifugation at 6000 RPM for 10 minutes. After centrifugation oleic acid coated Fe_3O_4 magnetic fluid was stored at room temperature.

3.2 Synthesis of $MnFe_2O_4$ (Manganese Ferrite) nanoparticles

Materials:

Ferric chloride Hexahydrate ($FeCl_3 .6H_2O$) and ($MnCl_2 .4H_2O$) are obtained from HIMEDIA are used as precursors. NaOH is used as a base and obtained from LOBA chemicals. All aqueous solutions are prepared in Milli-Q ultrapure distilled water (ρ = 18.2 MΩ).

Procedure:

All the precursors used are taken in the stoichiometric ratio of 1:2:8. Base fluid NaOH 0.8 mM (3.2 g) is prepared in 200 mL distilled water. Acids $FeCl_3.6H_2O$ 0.2 mM (5.406 g) and $MnCl_2.6H_2O$ 0.1 mM (1.979 g) are also prepared in 200 mL distilled water. Under the constant stirring acid solution is added to the base solution and pH is set to 11 within 10-15 seconds

with the help of excess NaOH solution. The reaction was allowed to proceed for 20 minutes at room temperature. The following reaction takes place:

0.2 mM $FeCl_3.6H_2O$ + 0.1 mM $MnCl_2.4H_2O$ + 0.8 mM NaOH $\rightarrow$ 0.1 mM $MnFe_2O_4$ + 0.8 mM NaCl + 2 mM H_2O

It is further continued at 90 ℃ for 3 hours. The precipitates are of brown color. The resultant slurry is magnetically decanted, washed with warm distilled water three to four times, and then treated with acetone to eliminate any contaminants, if any. After this, nanoparticles are dried overnight in oven at 60 ℃. The dried nanoparticles are then grinded using mortar pestle. Synthesis protocols followed here are summarized as a flow chart in Fig. 6.

Preparation of aqueous magnetic fluid of manganese ferrite

Manganese Ferrite ($MnFe_2O_4$) nanoparticles are synthesized by following the protocols described in Fig. 6, till the washing step. After multiple water washes, manganese ferrite nanoparticle are dispersed in 100 mL distilled water. Under basic circumstances, 2.3 g of oleic acid was dissolved to produce 100 mL of sodium oleate solution. 100 mL dispersion of manganese ferrite nanoparticles was then added to the sodium oleate solution (100 mL). It was stirred with the help of mechanical stirrer at room temperature for 2 hours. Following this it was heated to 90 ℃ for 2 minutes under continuous stirring. At this stage oleic acid binds to the surface of nanoparticles and stabilizes them by steric repulsion. Now the heating was turned off in order to allow the solution to cool to room temperature. Next to flocculate the nanoparticles, solution pH was adjusted to < 5 with the help of dil. HCl. It is then magnetically decanted and 3-4 times washed with warm distilled water. Following this the slurry was washed with ethanol + acetone (100 mL). After this nanoparticles are dispersed in 10 mL distilled water with sonication. Additional 15 mL sodium oleate solution was prepared as per the protocols explained previously. To the oleic acid-coated $MnFe_2O_4$ nanoparticle slurry, this sodium oleate solution was added drop by drop while being gently heated. Addition of oleic acid was continued drop - by - drop till nanoparticles exhibits complete suspension. Once it is fully suspended, addition of sodium oleate was stopped. To remove clusters of nanoparticles, if any; magnetic fluid thus prepared was subject to centrifugation at 6000 RPM for 10 minutes. After centrifugation oleic acid coated $MnFe_2O_4$ magnetic fluid was stored at room temperature.

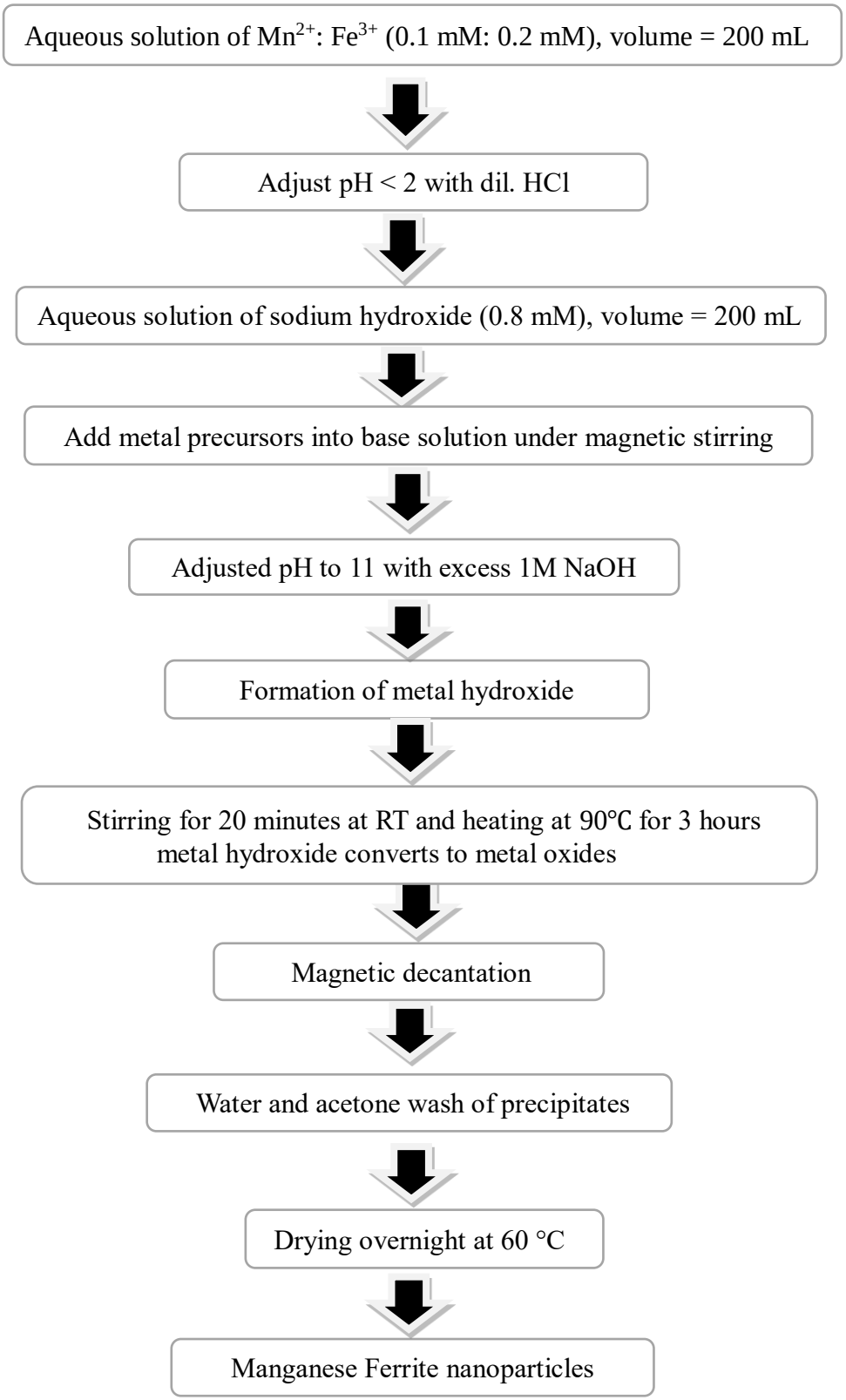

Fig. 6 Synthesis protocols for the preparation of $MnFe_2O_4$ nanoparticles

3.3 Synthesis of $CoFe_2O_4$ (Cobalt Ferrite) nanoparticles

Materials:

Ferric chloride Hexahydrate ($FeCl_3 .6H_2O$) obtained from HIMEDIA and Cobalt Chloride Hexahydrate ($CoCl_2 .6H_2O$) obtained from SD Fine chemicals limited are used as precursors. NaOH is used as a base and obtained from obtained from LOBA Chemicals. All aqueous solutions are prepared in Milli-Q ultrapure distilled water (ρ=18.2MΩ).

Procedure:

All the precursors used are taken in the stoichiometric ratio of 1:2:8. Base fluid NaOH 0.8 mM (3.2 g) is prepared in 200 mL distilled water. Acids $FeCl_3.6H_2O$ 0.2 mM (5.40 g) and $CoCl_2.6H_2O$ 0.1 mM (2.37 g) are also prepared in 200 mL distilled water. Under the constant stirring acid solution is added to the base solution and pH is set to 11 within 10-15 seconds with the help of excess NaOH solution. The reaction was allowed to proceed for 20 minutes at room temperature. Following reaction does take place:

0.2 mM $FeCl_3.6H_2O$ + 0.1 mM $CoCl_2 .6H_2O$ + 0.8 mM NaOH $\rightarrow$ 0.1 mM $CoFe_2O_4$ + 0.8 mM NaCl + 2.2 mM H_2O

Then the reaction is continued at 90 ℃ for 3 hours. The precipitates are of brown color. The obtained slurry is magnetically decanted and washed 3-4 times with warm distilled water followed by an acetone wash to remove impurities, if any. After this, nanoparticles are dried overnight in oven at 60 ℃. The dried nanoparticles are then grinded using mortar pestle. Synthesis protocols followed here are summarized as a flow chart in Fig. 7.

Preparation of aqueous magnetic fluid of cobalt ferrite

Cobalt ferrite ($CoFe_2O_4$) nanoparticles are synthesized by following the protocols described in Fig 7, till the washing step. . After multiple water wash, cobalt ferrite nanoparticle are dispersed in 100 mL distilled water. Under basic circumstances, 2.3 g of oleic acid was dissolved to produce 100 mL of sodium oleate solution. 100 mL dispersion of cobalt ferrite nanoparticles was then added to the sodium oleate solution (100 mL). It was stirred with the help of mechanical stirrer at room temperature for 2 hours. Following this it was heated to 90 ℃ for 2 minutes under continuous stirring.

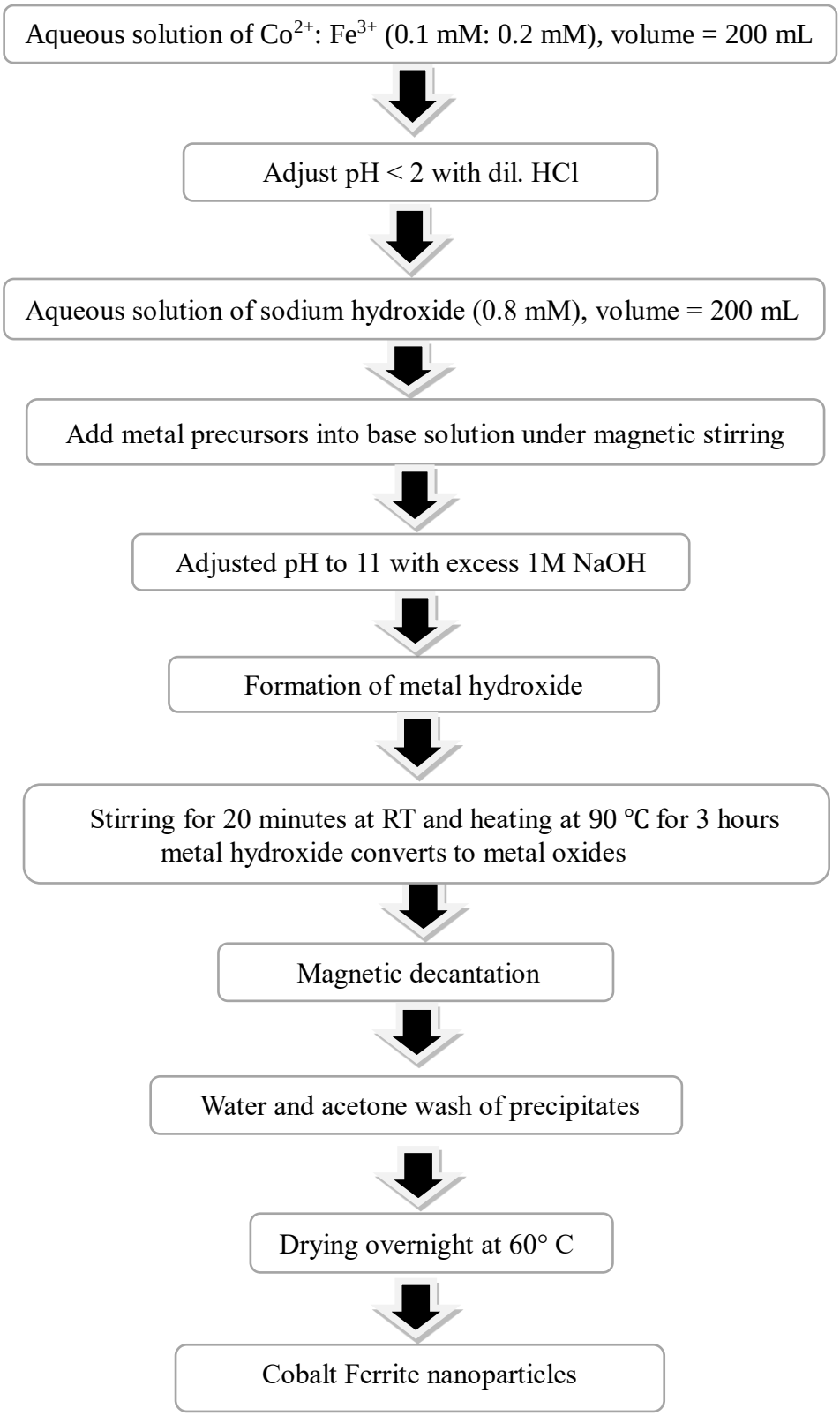

Fig. 7 Synthesis protocols for the preparation of $CoFe_2O_4$ nanoparticles

At this stage oleic acid binds to the surface of nanoparticles and stabilizes them by steric repulsion. Now the heating was turned off in order to allow the solution to cool to room temperature. Next to flocculate the nanoparticles, solution pH was adjusted to < 5 with the help of dil. HCl. It is then magnetically decanted and 3-4 times washed with warm distilled water. Following this the slurry was washed with ethanol + acetone (100 mL). After this nanoparticles are dispersed in 10 mL distilled water with sonication. Additional 15 mL sodium oleate solution was prepared as per the protocols explained previously. To the oleic acid-coated $CoFe_2O_4$ nanoparticle slurry, this sodium oleate solution was added drop by drop while being gently heated. Addition of oleic acid was continued drop - by - drop till nanoparticles exhibits complete suspension. Once it is fully suspended, addition of sodium oleate was stopped. To remove clusters of nanoparticles, if any; magnetic fluid thus prepared was subject to centrifugation at 6000 RPM for 10 minutes. After centrifugation oleic acid coated $CoFe_2O_4$ magnetic fluid was stored at room temperature.

AFe_2O_4 (A = Fe, Mn, Co) nanoparticles / magnetic fluids were characterized by the following techniques:

1) X-Ray diffraction
2) Vibrating sample magnetometer
3) Dynamic light scattering
4) Magnetic hyperthermia

4.1 X-Ray Diffraction

By using powder x-ray diffraction (XRD), magnetic nanoparticles crystal structure have been investigated. XRD patterns are recorded on Rigaku Smart lab SE powder X-ray diffractometer. XRD patterns of as-synthesized AFe_2O_4 (A = Fe, Mn, Co) nanoparticles are shown in Fig. 8. The XRD patterns are recorded in the 2Θ range of 20º-80º using CuKα monochromatic radiation (λ = 1.54 Å). All the six peaks observed in the diffractograms are indexed well with the cubic inverse spinel structure [36].

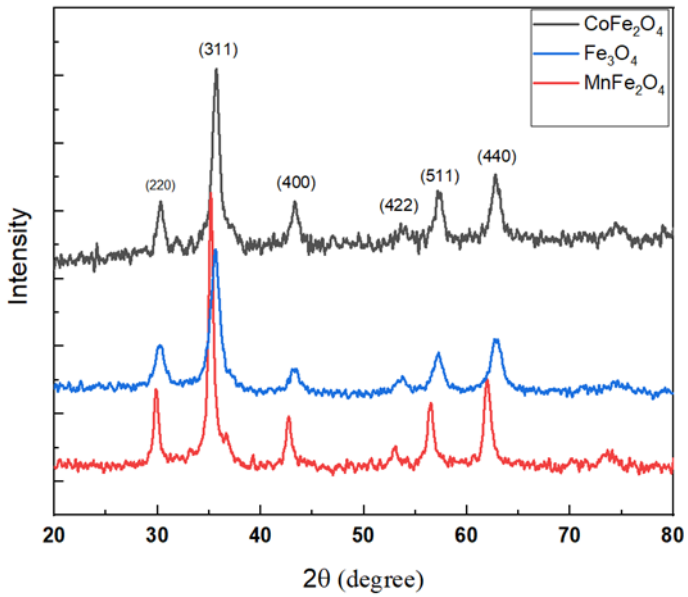

Fig. 8 XRD patterns of AFe_2O_4 (A=Fe, Mn, Co) nanoparticles

The peaks observed at 2θ values: 29°, 35°, 43°, 52°, 62° corresponds to (220), (311), (400), (422), (511), (440) crystal planes of FCC structure. No extra peak was detected, indicating high purity of the synthesized particles. The crystallite size was calculated from

the highest intense peak (311) by using Debye-Scherer formula

$$d = \frac{0.9\lambda}{\beta \cos\theta}$$

Here, d = crystallite size, λ =wavelength of x-ray source (λ=1.54Å), β = full width at half maximum (FWHM) of highest intense peak determined by fitting it with pseudo-voigt function, θ = diffraction angle of highest intense reflection.

Table 1 lists the computed crystallite size for each sample. The size of the crystallite was determined to be between 7 and 16 nm. Nanoparticles with extremely small crystallite sizes may exhibit superparamagnetic properties. The following equations have been used to compute the lattice parameter "a" and the inter planer distance "d_{hkl}" according to Bragg's law.

$$2d\sin\Theta = n\lambda$$

$$d = \frac{a}{\sqrt{h^2 + k^2 + l^2}}$$

Here, d is inter planer spacing, a is lattice parameter, and h, k, l are miller indices

Table 1: Crystallite size and lattice parameters of AFe2O4 (A = Fe, Mn, Co) nanoparticles

Sample	**Lattice parameter (a) (Å)**	**Crystallite size (nm)**
Fe_3O_4	8.35	7.7
$MnFe_2O_4$	8.38	15.3
$CoFe_2O_4$	8.32	10.6

The estimated lattice parameter values of the synthesized samples correlate well with the reported values for the JCPDS card number. 00-001-1121 ($CoFe_2O_4$), 01-088-0315 (Fe_3O_4) and 98-002-4073 ($MnFe_2O_4$).

4.2 Vibrating Sample Magnetometer Analysis

At room temperature, magnetization measurements of AFe_2O_4 (A=Fe, Mn, Co) nanoparticles are performed using a Lake Shore 7404 vibrating sample magnetometer. M-H hysteresis loops are shown by Fig. 9. Measurements were carried out in the field range of -10 to +10 KOe. AFe_2O_4 (A=Fe, Mn, Co) nanoparticles possess soft ferromagnetic behavior as evidence from their M-H loops. Fe_3O_4 and $MnFe_2O_4$ exhibits superparamagnetic behavior demonstrated by extremely low coercivity and remanence. $CoFe_2O_4$ exhibits soft ferromagnetic behavior. Table 2 shows the saturation magnetization, remnant magnetization and coercivity of AFe_2O_4 (A=Fe, Mn, Co) nanoparticles. Saturation Magnetization of NPs varies between 40 emu/gm to 50 emu/gm. The coercivity and remanence increases with the increase in the crystallite size [30].

Table 2: Magnetic properties of AFe_2O_4 (A=Fe, Mn, Co) nanoparticles

Sample	Saturation magnetization (emu/gm)	Remnant magnetization (emu/gm)	Coercivity (Oe)
Fe_3O_4	48.13	2.60	49
$MnFe_2O_4$	40.40	2.60	35
$CoFe_2O_4$	44.13	10.10	440

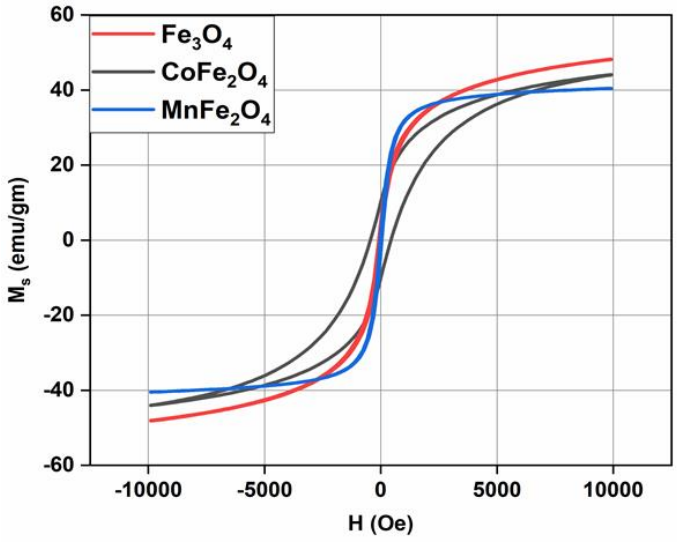

Fig. 9 M-H hysteresis loops of AFe_2O_4 (A=Fe, Mn, Co) NPs

4.3 Hydrodynamic Particle size analysis

Hydrodynamic size and size distribution of AFe_2O_4 (A=Fe, Mn, Co) nanoparticles with bilayer coating of oleic acid, which are dispersed in water has been determined by dynamic light scattering. The measurements were made using the Brookhaven 90 Plus particle size analyzer at room temperature by using 633 nm laser. Figures 10 (a), (b) and (c) show the size distribution histograms of AFe_2O_4 (A=Fe, Mn, Co) nanoparticles. Mean hydrodynamic sizes and polydispersity indices of AFe_2O_4 (A=Fe, Mn, Co) nanoparticles are listed in Table 3.

Table 3: Hydrodynamic size and polydispersity index of AFe_2O_4 (A=Fe, Mn, Co) nanoparticles

Sample	Hydrodynamic size (nm)	Polydispersity Index
Fe_3O_4	122	0.17
$MnFe_2O_4$	179	0.34
$CoFe_2O_4$	132	0.23

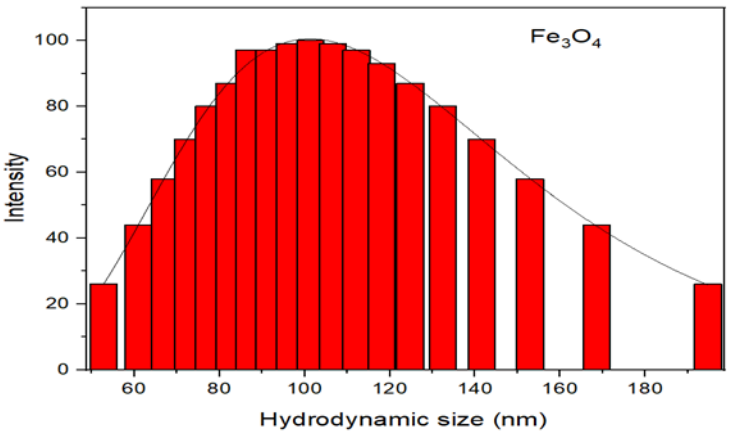

Fig. 10 (a) Hydrodynamic particle size distribution of Fe_3O_4 nanoparticles fitted with lognormal size distribution function

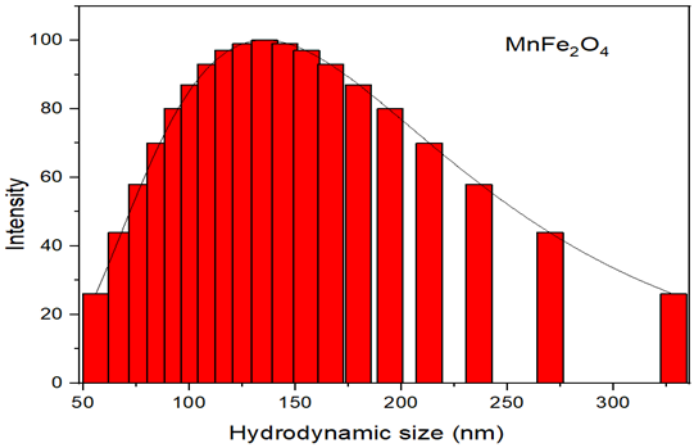

Fig. 10 (b) Hydrodynamic particle size distribution of $MnFe_2O_4$ nanoparticles fitted with lognormal size distribution function

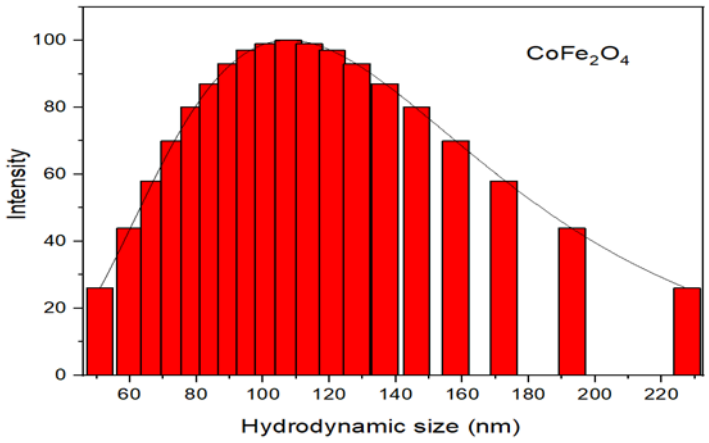

Fig 10 (c) Hydrodynamic particle size distributions of $CoFe_2O_4$ nanoparticles fitted with lognormal size distribution function

4.4 Magnetic Hyperthermia

We have evaluated magnetic hyperthermia efficiency of water based magnetic fluids of AFe_2O_4 (A=Fe, Mn, Co) nanoparticles by measuring time versus temperature plots on nanotherics magnetherm magnetic hyperthermia setup. Magnetic nanoparticles concentrations in magnetic fluids were 70 mg/mL for Fe_3O_4, 200 mg/mL for $MnFe_2O_4$ and 60 mg/mL for $CoFe_2O_4$. Magnetic hyperthermia measurements were performed as a function of magnetic field strength (2-10 mT) and field frequency (162-935.6 kHz) for 10 minutes. MNPs exhibits highest SAR values for 10 mT field strength at 935.6 kHz field frequency. Amongst the tested MNPs, Fe_3O_4 possess the highest SAR value (27.35 W/g), followed by $MnFe_2O_4$ (1.91 W/g) and $CoFe_2O_4$ (0.94 W/g).

4.4.1 Magnetic hyperthermia of Iron Oxide nanoparticles

Figure 14 shows that magnetic hyperthermia results of Fe_3O_4 nanoparticles measured at 580.6 kHz frequency and 8 mT field at different nanoparticle concentrations. The heat rise at higher concentration is above 90 °C in 360 sec. As the concentration becomes low the heat rise also becomes slow. Time Temperature graph plotted at 580.6 kHz frequency and 8 mT fields produce enough temperature in less time that is required (45°C) for magnetic hyperthermia treatment.

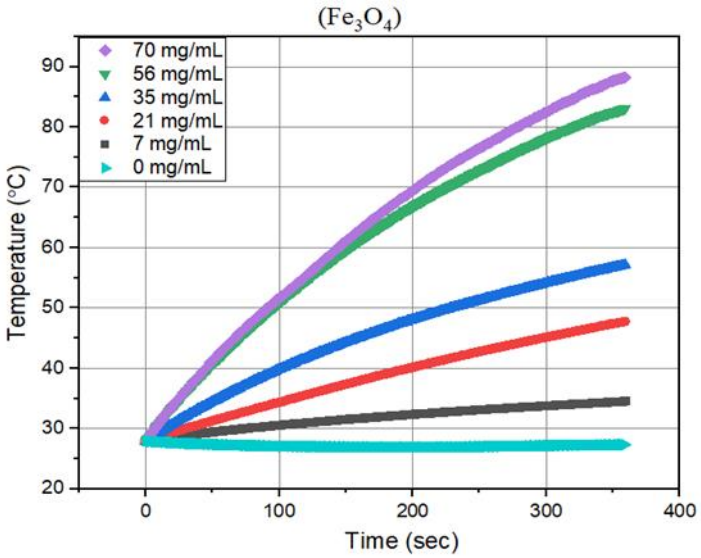

Fig.11 Temperature- time plots of Fe_3O_4 nanoparticles measured at 580.6 kHz frequency and 8 mT field for different nanoparticle concentrations

SAR (W/g) values for Fe_3O_4 nanoparticles is calculated by using corrective slope method at different fields and frequencies and mentioned in Fig. 12.

$$\text{SAR (W/g)} = C\frac{\Delta T}{\Delta t}$$

Her C is the specific heat capacity of colloid (here C is taken for water) and $\Delta T/\Delta t$ is the rate of change of temperature. Figure 12 show that SAR changes with change in applied field as well as with frequency. SAR increases as we go towards higher frequency and field.

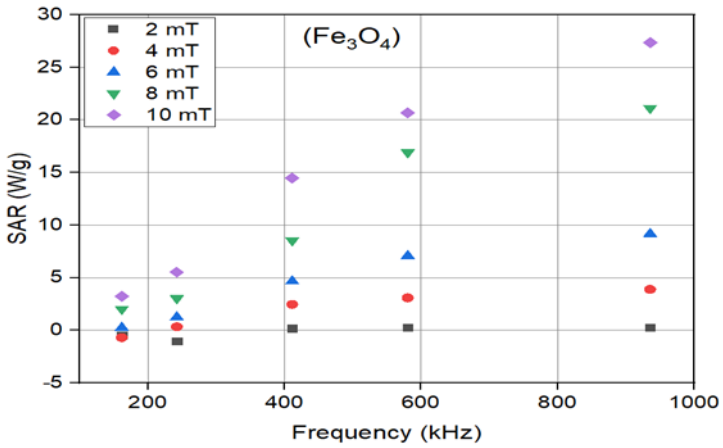

Fig. 12 SAR values of Fe_3O_4 nanoparticles measured at different frequencies and different fields at an constant concentration of 70 mg/mL.

4.4.2 Magnetic hyperthermia of Manganese Ferrite nanoparticles

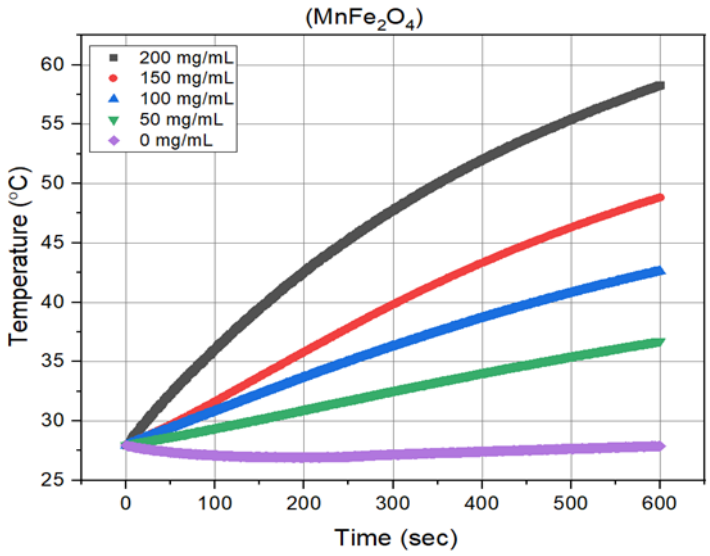

Fig.13 Temperature- time plots of $MnFe_2O_4$ nanoparticles measured at 935.6 kHz frequency and 10 mT field for different nanoparticle concentrations

Figure 13 shows temperature – time plots of $MnFe_2O_4$ nanoparticles measured at 935.6 kHz frequency and 10 mT field at different concentrations. The heat rise at higher concentration is nearly 60 °C in 600 sec. As the concentration gets lower the heat rise also becomes sluggish. It shows that 935.6 KHz frequency and 10 mT fields is enough to reach the magnetic hyperthermia temperature. The concentration of $MnFe_2O_4$ nanoparticles is 200 mg/mL and the temperature rise as compared to Fe_3O_4 nanoparticles is low.

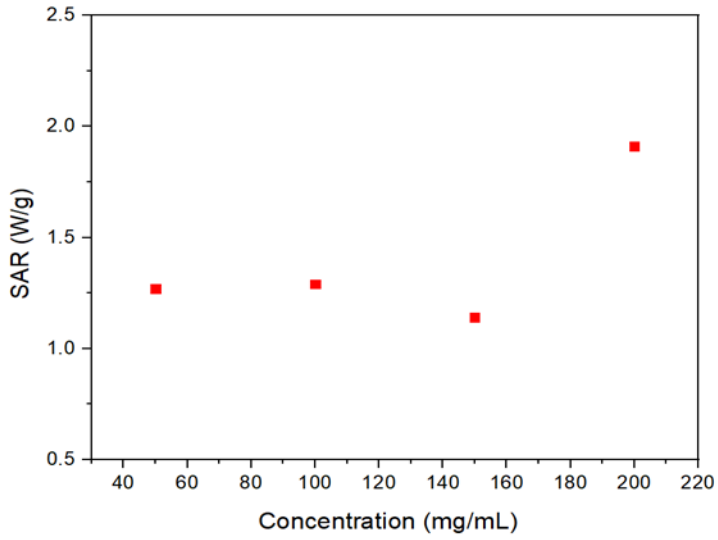

Fig.14 Effect of nanoparticle concentration on SAR values measured at 10 mT field and 935.6 kHz frequency

Figure 14 shows changes in SAR values as a function of nanoparticle concentration measured at 935.6 kHz frequency and 10 mT field. No significant change is observed in the SAR values of when different nanoparticle concentrations were used in the study.

4.4.3 Magnetic hyperthermia of Cobalt Ferrite nanoparticles

The synthesized cobalt ferrite has a concentration of 60 mg/mL. Hyperthermia experiments were carried out at highest available frequency (935.6 kHz) and field (10 mT) for synthesized fluid. However, the desired temperature (45 °C) could not be achieved with the test conditions. Maximum temperature rise was 8 °C and corresponding SAR value was 0.94 W/g.

4.5 Conclusions

AFe_2O_4 (A=Fe, Mn, Co) nanoparticles are prepared by chemical co-precipitation method. The average crystallite size of AFe_2O_4 (A=Fe, Mn, Co) found to be in the range of 7-16 nm. A study using a vibrating sample magnetometer showed that AFe_2O_4 NPs exhibit soft ferrite behavior and had saturation magnetism between (40-50) emu/g. Dynamic light scattering shows that average hydrodynamic size of AFe_2O_4 (A=Fe, Mn, Co) nanoparticles is in the range of 120 nm to180 nm. SAR values of AFe_2O_4 (A=Fe, Mn, Co) nanoparticles increases with increase in field strength and frequency and it is independent of nanoparticle concentration. Highest SAR values observed for AFe_2O_4 (A=Fe, Mn, Co) is 27.35 W/g for Fe_3O_4, followed by 1.91 W/g for

$MnFe_2O_4$ and 0.94 W/g for $CoFe_2O_4$ at 10 mT field strength and 935.6 KHz field frequency. Amongst the three ferrites, Fe_3O_4 is most appropriate for magnetic hyperthermia studies as it possess highest temperature rise at lower nanoparticle concentration.

References

1. Kalyankar T. M., Butle S. R., Chamwad G. N. Application of Nanotechnology in Cancer Treatment. Research J. Pharm. and Tech. 5(9): September 2012; Page 1161-1167.
2. Mansoori, G. Ali. Principles of nanotechnology: molecular-based study of condensed matter in small systems. World Scientific, 2005.
3. Lin, Patrick, Daniel Moore, and Fritz Allhoff. What is nanotechnology and why does it matter: from science to ethics. John Wiley & Sons, 2009.
4. Jeevanandam, Jaison et al. "Review on nanoparticles and nanostructured materials: history, sources, toxicity and regulations." Beilstein journal of nanotechnology vol. 9 1050-1074. 3 Apr. 2018.
5. Naik, H., et al. "Socioeconomic status and lifestyle behaviours in cancer survivors: smoking and physical activity." Current Oncology 23.6 (2016): 546-555.
6. Gavas, Shreelaxmi, Sameer Quazi, and Tomasz M. Karpiński. "Nanoparticles for cancer therapy: Current progress and challenges." Nanoscale Research Letters 16.1 (2021): 1-21.
7. Sudhakar, Akulapalli. "History of cancer, ancient and modern treatment methods." Journal of cancer science & therapy 1.2 (2009): 1.
8. https://www.cancer.gov/about-cancer/treatment/types (NIH).
9. Wu et al., Journal of Cancer Molecules 2006, 2(2) 57-66
10. American Cancer Society (ACS). Hyperthermia 2009, Available at URL address: http://www.cancer.org/docroot/ETO/content/ETO 1 2x Hyperthermia.asp
11. https://www.motioncontroltips.com/hysteresis-loss/.
12. Nandhini, G., and M. K. Shobana. "Role of ferrite nanoparticles in hyperthermia applications." Journal of Magnetism and Magnetic Materials 552 (2022): 169236.
13. Chou, Chung-Kwang. "Use of heating rate and specific absorption rate in the hyperthermia clinic." International journal of hyperthermia 6.2 (1990): 367-370.
14. Sangaa, Deleg, et al. "An Overview of Investigation for Ferrite Magnetic Nanomaterial." Solid State Phenomena, vol. 271, Trans Tech Publications, Ltd., Jan. 2018, pp. 51–63. Crossref, doi:10.4028/www.scientific.net/ssp.271.51.
15. https://en.wikipedia.org/wiki/Ferrite_(magnet)
16. Cabuy, Erik. (2011). Hyperthermia in cancer treatment. Reliable Cancer Therapies. 1. 1-48.
17. Issa, Bashar, et al. "Magnetic nanoparticles: surface effects and properties related to biomedicine applications." International journal of molecular sciences 14.11 (2013): 21266-21305.
18. https://www.science20.com/mei/blog/blocking_temperature
19. https://www.researchgate.net/figure/Oleic-acid-left-and-its-linkage-with-iron-oxide-nanoparticle-right_fig2_265139527
20. http://rasayanjournal.co.in/admin/php/upload/547_pdf.pdf

21. https://www.cancer.gov/aboutcancer/treatment/types/hyperthermia#:~:text=Hyperthermia%20treatment%20research,What%20is%20hyperthermia%20treatment%3F,%2C%20thermal%20ablation%2C%20or%20thermotherapy
22. SWT Physics Department. "Vibrating Sample Magnetometer" (PDF).]
23. Hofmann, H., et al. "Superparamagnetic iron oxide nanoparticles for multiple biomedical applications." Nanotechnology 1 (2005): 152-155.
24. Drake, Philip, et al. "Gd-doped iron-oxide nanoparticles for tumour therapy via magnetic field hyperthermia." Journal of Materials Chemistry 17.46 (2007): 4914-4918.
25. Hadjipanayis, Costas G., et al. "Metallic iron nanoparticles for MRI contrast enhancement and local hyperthermia." Small 4.11 (2008): 1925-1929.
26. Soares, Paula IP, et al. "Iron oxide nanoparticles stabilized with a bilayer of oleic acid for magnetic hyperthermia and MRI applications." Applied Surface Science 383 (2016): 240-247.
27. Ebrahimisadr, Saeid, Bagher Aslibeiki, and Reza Asadi. "Magnetic hyperthermia properties of iron oxide nanoparticles: The effect of concentration." Physica C: Superconductivity and its applications 549 (2018): 119-121.
28. Bani, Milad Salimi, et al. "Casein-coated iron oxide nanoparticles for in vitro hyperthermia for cancer therapy." Spin. Vol. 9. No. 02. World Scientific Publishing Company, 2019.
29. Mozaffari, Mortaza, Behshid Behdadfar, and Jamshid Amighian. "Preparation and characterization of manganese ferrite nanoparticles via co-precipitation method for hyperthermia." Iranian Journal of Pharmaceutical Sciences 4.2 (2008): 115-118.
30. Doaga, A., et al. "Synthesis and characterizations of manganese ferrites for hyperthermia applications." *Materials Chemistry and Physics* 143.1 (2013): 305-310.
31. Patade, Supriya R., et al. "Effect of zinc doping on water-based manganese ferrite nanofluids for magnetic hyperthermia application." *AIP Conference Proceedings*. Vol. 2265. No. 1. AIP Publishing LLC, 2020.
32. Mazario, Eva, et al. "Magnetic hyperthermia properties of electrosynthesized cobalt ferrite nanoparticles." *The journal of physical chemistry c* 117.21 (2013): 11405-11411.
33. Al Lehyani, S. H. A., et al. "Magnetic hyperthermia using cobalt ferrite nanoparticles: the influence of particle size." *Int. J. Adv. Technol* 8 (2017): 567-579.
34. Jose, J., Kumar, R., Harilal, S. *et al.* Magnetic nanoparticles for hyperthermia in cancer treatment: an emerging tool. *Environ Sci Pollut Res* **27,** 19214–19225 (2020).
35. https://serc.carleton.edu/research_education/geochemsheets/BraggsLaw.html
36. https://www.unf.edu/~michael.lufaso/chem4627/ch8_solid_state.pdf
37. Kaur, Navjot, and Bhupendra Chudasama. "Tunable Curie temperature of Mn0. 6Zn0. 4Fe2O4 nanoparticles." Journal of Magnetism and Magnetic Materials 465 (2018): 164-168.
38. Kaur, Navjot, and Bhupendra Chudasama. "Effect of thermal aging on stability of transformer oil based temperature sensitive magnetic fluids." Journal of Magnetism and Magnetic Materials 451 (2018): 647-653.
39. Kaur, Navjot, and Bhupendra Chudasama. "Colloidal stability of Mn1− x Znx Fe2O4 nanoparticles in transformer oil: role of Zn substitution." Micro & Nano Letters 14.6 (2019): 609-612.
40. Kaur, Navjot, and Bhupendra Chudasama. "Effect of hydrodynamic size on colloidal stability and lifetime of Mn-Zn magnetic fluids." Colloid and Polymer Science 297.11 (2019): 1403-1409.
41. Kareem, Sahira Hassan, et al. "Influence of zinc on the structure and morphology of manganese ferrite nanoparticles." Jurnal Teknologi 69.5 (2014).

42. Joseyphus, R. Justin, et al. "Synthesis and magnetic properties of the size-controlled Mn–Zn ferrite nanoparticles by oxidation method." Journal of Physics and Chemistry of Solids 67.7 (2006): 1510-1517.
43. Costa, A. C. F. M., et al. "Synthesis, microstructure and magnetic properties of Ni–Zn ferrites." Journal of magnetism and magnetic materials 256.1-3 (2003): 174-182.
44. Tang, Z. X., et al. "Preparation of manganese ferrite fine particles from aqueous solution." Journal of colloid and interface science 146.1 (1991): 38-52.
45. Puspitasari, Poppy, Alief Muhammad, and Heru Suryanto. "Determination of the magnetic properties of manganese ferrite by the coprecipitation method at different pH concentrations." High Temperature Material Processes: An International Quarterly of High-Technology Plasma Processes 22.4 (2018).
46. Zipare, Kisan, et al. "Superparamagnetic manganese ferrite nanoparticles: synthesis and magnetic properties." Journal of Nanoscience and Nanoengineering 1.3 (2015): 178-182.
47. Irfan, Elahi, et al. "Co-precipitation synthesis, physical and magnetic properties of manganese ferrite powder." African journal of pure and applied chemistry 6.1 (2012): 1-5.
48. Sharma, Uma Shankar, Ram Naresh Sharma, and Rashmi Shah. "Physical and magnetic properties of manganese ferrite nanoparticles." International Journal of Engineering Research and Applications 4.8 (2014): 14-17.
49. Patade, Supriya R., et al. "Effect of zinc doping on water-based manganese ferrite nanofluids for magnetic hyperthermia application." AIP Conference Proceedings. Vol. 2265. No. 1. AIP Publishing LLC, 2020.
50. Kaur, Navjot, and Bhupendra Chudasama. "Structure induced tunable magnetic properties of Zn substituted Mn1− xZnx Fe2O4 (x= 0–1) NPs." Micro & Nano Letters 12.3 (2017): 151-156.
51. Patade, Supriya R., et al. "Self-heating evaluation of superparamagnetic MnFe2O4 nanoparticles for magnetic fluid hyperthermia application towards cancer treatment." Ceramics International 46.16 (2020): 25576-25583.
52. Yashpreet, and Bhupendra Chudasama. "Effect of annealing on structural and magnetic properties of manganese ferrite nanoparticles." AIP Conference Proceedings. Vol. 2265. No. 1. AIP Publishing LLC, 2020.
53. Besenhard, Maximilian O., et al. "Co-precipitation synthesis of stable iron oxide nanoparticles with NaOH: New insights and continuous production via flow chemistry." Chemical Engineering Journal 399 (2020): 125740.
54. Salimi, Marzieh, et al. "Treatment of breast cancer-bearing BALB/c mice with magnetic hyperthermia using dendrimer functionalized iron-oxide nanoparticles." Nanomaterials 10.11 (2020): 2310.
55. Ng, Eddie Yin Kwee, and Srinivasan Dinesh Kumar. "Physical mechanism and modeling of heat generation and transfer in magnetic fluid hyperthermia through Néelian and Brownian relaxation: a review." Biomedical engineering online 16.1 (2017): 1-22.
56. Mathew, Daliya S., and Ruey-Shin Juang. "An overview of the structure and magnetism of spinel ferrite nanoparticles and their synthesis in microemulsions." Chemical engineering journal 129.1-3 (2007): 51-65.
57. Gutiérrez, Lucía, et al. "Synthesis methods to prepare single-and multi-core iron oxide nanoparticles for biomedical applications." Dalton Transactions 44.7 (2015): 2943-2952.
58. Baig, Nadeem, Irshad Kammakakam, and Wail Falath. "Nanomaterials: A review of synthesis methods, properties, recent progress, and challenges." Materials Advances 2.6 (2021): 1821-1871.
59. Houshiar, Mahboubeh, et al. "Synthesis of cobalt ferrite (CoFe2O4) nanoparticles using combustion, coprecipitation, and precipitation methods: A comparison study of size,

structural, and magnetic properties." Journal of Magnetism and Magnetic Materials 371 (2014): 43-48.
60. Gul, I. H., et al. "Optical, magnetic and electrical investigation of cobalt ferrite nanoparticles synthesized by co-precipitation route." Journal of alloys and compounds 507.1 (2010): 201-206.
61. El-Okr, M. M., et al. "Synthesis of cobalt ferrite nano-particles and their magnetic characterization." Journal of Magnetism and Magnetic Materials 323.7 (2011): 920-926.

Turnitin Originality Report

Processed on: 26-Jul-2022 03:33 IST
ID: 1875174578
Word Count: 6296
Submitted: 1

Abhishek thesis By Abhishek Chandel

Similarity Index	Similarity by Source	
11%	Internet Sources	6%
	Publications	6%
	Student Papers	4%

2% match (Internet from 02-Jul-2022)
https://tudr.thapar.edu:8080/jspui/bitstream/10266/5868/1/merged%20thesis%20navjot.pdf

1% match (publications)
A. Doaga, A.M. Cojocariu, W. Amin, F. Heib, P. Bender, R. Hempelmann, O.F. Caltun. "Synthesis and characterizations of manganese ferrites for hyperthermia applications", Materials Chemistry and Physics, 2013

1% match (student papers from 16-Jul-2017)
Submitted to Thapar University, Patiala on 2017-07-16

1% match (publications)
Supriya R. Patade, Deepali D. Andhare, Sandeep B. Somvanshi, Prashant B. Kharat, K. M. Jadhav. "Effect of zinc doping on water-based manganese ferrite nanofluids for magnetic hyperthermia application", AIP Publishing, 2020

1% match (Internet from 05-Mar-2021)
https://archive.org/details/peel?and%5B%5D=firstCreator%3Al&sort=creatorSorter

1% match (publications)
Saeid Ebrahimisadr, Bagher Aslibeiki, Reza Asadi. "Magnetic hyperthermia properties of iron oxide nanoparticles: The effect of concentration", Physica C: Superconductivity and its Applications, 2018

< 1% match (student papers from 18-Jul-2018)
Submitted to Thapar University, Patiala on 2018-07-18

< 1% match (Internet from 29-Sep-2020)
https://www.mdpi.com/1422-0067/14/8/15977/htm

< 1% match (publications)
Milad Salimi Bani, Shadie Hatamie, Mohammad Haghpanahi, Hossein Bahreinizad et al. " Casein-Coated Iron Oxide Nanoparticles for Hyperthermia for Cancer Therapy ", SPIN, 2019

< 1% match (Internet from 07-Feb-2022)
https://cyberleninka.org/article/n/1253155

< 1% match (publications)
Kaan Yilancioglu, Murat Cokol, Inanc Pastirmaci, Batu Erman, Selim Cetiner. "Oxidative Stress Is a Mediator for Increased Lipid Accumulation in a Newly Isolated Dunaliella salina Strain", PLoS ONE, 2014